

Exact diagonalization results for resonant inelastic x-ray scattering spectra of one-dimensional Mott insulators

Stefanos Kourtis, Jeroen van den Brink, and Maria Daghofer

Institute for Theoretical Solid State Physics, IFW Dresden, 01171 Dresden, Germany

(Received 28 November 2011; published 29 February 2012)

We examine the momentum-dependent excitation spectra of indirect as well as direct resonant inelastic x-ray scattering (RIXS) processes in half-filled (extended) Hubbard rings. We determine the fundamental features of the ground-state RIXS response and discuss the experimental conditions that can allow for the low-energy part of these features to be distinguished in one-dimensional copper-oxide materials, focusing particularly on the different magnetic excitations occurring in indirect and direct RIXS processes. We study the dependence of spin and charge excitations on the choice of and detuning from resonance. Moreover, final-state excitation weights are calculated as a function of the core-hole potential strength and lifetime. We show that these results can be used to determine material characteristics, such as the core-hole properties, from RIXS measurements.

DOI: [10.1103/PhysRevB.85.064423](https://doi.org/10.1103/PhysRevB.85.064423)

PACS number(s): 78.20.Bh, 71.10.Fd, 72.10.Di, 78.70.Ck

I. INTRODUCTION

Strongly interacting one-dimensional (1D) quantum systems provide the opportunity to observe distinctive signatures of theoretical predictions, such as the separation of fermionic excitations into charge and spin components.¹ Prototypical materials that exhibit 1D behavior are the corner-sharing copper-oxide compounds Sr_2CuO_3 and SrCuO_2 , in which three-dimensional (3D) antiferromagnetic correlations disappear above a temperature T_N of a few Kelvin, and the majority of electronic properties come from electrons moving on almost independent chains. A variety of experimental techniques have been used to verify the 1D character of the excitations in these materials^{2–6} and the existence of the expected spin-charge separation.^{7–10} These observations have induced further interest in cross examining the results of different experimental probes in order to test the quantitative agreement with theoretical descriptions of the underlying quantum mechanical processes.

Resonant inelastic x-ray scattering (RIXS) is a particularly promising technique for research in this direction since it can probe multiple spin and charge excitations on the same footing.¹¹ In RIXS, incident x-ray photons are used that have a frequency close to the corresponding excitation energy for the promotion of a core electron to an empty state in or above the valence orbital of interest, the two alternatives defining direct and indirect RIXS, respectively.^{12,13} In the intermediate state, the resulting core hole perturbs the valence electron system locally until an electron decays into the empty core state, emitting an x-ray photon shifted in energy, momentum, and polarization with respect to the incoming one. RIXS experiments at the Cu K edge have been performed on the aforementioned 1D cuprates,^{14–18} and the dominant spectral features have been attributed to d - d excitations. Spin excitations were not distinguished in the earlier experiments because of resolution limitations of the instrumentation used. These limitations can be overcome in today's experimental setups, as has been demonstrated by the observation of spin excitations in other 1D (Ref. 19) or 2D (Refs. 20 and 21) cuprates and iridates,^{11,22,23} although RIXS measurements for the simpler Sr-based chain cuprates are still awaited.²⁴

The distinct form of the theoretical expression for the RIXS cross section provides a unique way to study properties of models for one-dimensional condensed matter systems. The shortness of the intermediate-state lifetime has been exploited to perform expansions for the magnetic indirect RIXS cross section of Mott insulators.^{25–27} The case of magnetic excitations in direct RIXS has been investigated in this manner²⁸ and also by an effective operator method,²⁹ recently applied to the case of the quasi-1D compound TiOCl .³⁰ Apart from model fits to experimental data,^{15,16} exact numerical investigations of indirect RIXS on small systems have been performed for the 1D (extended) Hubbard,³¹ Heisenberg,^{32,33} t - J ,³³ and dp (Ref. 34) models, whereas only a calculation of direct RIXS spectra for the Heisenberg and t - J models has appeared so far.³³ Furthermore, in the existing works, only the momentum dependence of RIXS spectra at specific resonance conditions has been obtained. It has been established experimentally that the character of excitations present in the final state of RIXS depends strongly on the detuning from resonance. Therefore, it is of interest to determine the effect of detuning on final-state excitations in a generic model and see how it compares to the behavior of real systems. Moreover, the effect of the intermediate-state core hole, which will play an increasingly important role with the advent of time-resolved RIXS experiments, has been considered only heuristically so far.

The purpose of this paper is to present a systematic numerical study of both indirect and direct RIXS processes in a 1D Mott-insulating system. To this end, the Lanczos exact diagonalization method is used to calculate the RIXS spectra for the Hubbard and extended Hubbard models at half-filling. The focus is on determining fundamental properties and extracting trends of the models under changes in the core-hole parameters rather than fitting experimental data. However, as the (extended) Hubbard model is believed to capture the essential physics of 1D chain cuprates at low energies, our results should be adequate to make qualitative predictions for the experimental outcome in this energy range. In Sec. II, the theoretical formulation leading to the evaluated RIXS cross section is briefly reviewed. In Sec. III, the RIXS response is calculated as a function of incoming photon energy. Moreover,

the dependence of the RIXS spectra upon the values of core-hole potential and lifetime is carefully investigated, and it is shown how the core-hole parameters can be related to direct RIXS experiments. Our conclusions are summarized in Sec. IV.

II. RIXS CROSS SECTION

A. Kramers-Heisenberg formula

The unperturbed Hamiltonian \hat{H}_0 of choice for the N -site, 1D system we wish to study is the single-band Hubbard model

$$\hat{H}_0 = -t \sum_{j\sigma} (c_{j\sigma}^\dagger c_{j+1\sigma} + \text{H.c.}) + U \sum_j \hat{n}_{j\uparrow} \hat{n}_{j\downarrow}, \quad (1)$$

where $c_{j\sigma}^\dagger$ creates electrons with spin σ at site j , $\hat{n}_{j\sigma} = c_{j\sigma}^\dagger c_{j\sigma}$, t is the hopping integral, and U the onsite Coulomb repulsion strength. In one dimension, any nonzero U/t ratio is enough to guarantee a Mott-insulator ground state with energy E_g at half-filling.¹ For comparison, we also study the extended Hubbard model with an additional nearest-neighbor interaction

$$\hat{H}_{\text{ext}} = \hat{H}_0 + V \sum_{j\sigma\sigma'} \hat{n}_{j\sigma} \hat{n}_{j+1\sigma'} \quad (2)$$

with $V = 2t$. The core hole present in the intermediate state acts as a localized potential scatterer for the $3d$ electrons and can be expressed as

$$\hat{H}_{\text{int}} = -V_c \sum_{j\sigma\sigma'} \hat{n}_{j\sigma} \hat{n}_{j\sigma'}^h, \quad (3)$$

where $\hat{n}_{j\sigma}^h$ is the number operator for core holes, $\hat{n}_{j\sigma}^h = 1$ signifying the presence of a core hole with spin σ on site j . The core hole interacts via an attractive force parametrized by $V_c > 0$ with the total density $\hat{n}_j = \hat{n}_{j\uparrow} + \hat{n}_{j\downarrow}$ in the valence band described by \hat{H}_0 . The dipole operator that creates the intermediate state, as schematically illustrated in Fig. 1, is given by

$$\hat{D} = \sum_{j\sigma} e^{ikR_j} d_{j\sigma}^\dagger h_{j\sigma}, \quad (4)$$

where $h_{j\sigma}$ creates a core hole and $d_{j\sigma}^\dagger$ a photoexcited electron at position R_j ; k is the incoming photon momentum, corresponding to frequency ω_k . Here, we do not consider photon polarizations and geometrical factors. The RIXS cross section is given by the Kramers-Heisenberg formula³⁵

$$w \propto \sum_f |F_{fg}|^2 \delta(E_f - E_g - \Delta\omega), \quad (5)$$

where the sum is over all final states $|f\rangle$ with energies E_f . The RIXS amplitude has been defined as

$$F_{fg}(\omega_{\text{in}}) \equiv \sum_n \frac{\langle f | \hat{D}^\dagger | n \rangle \langle n | \hat{D} | g \rangle}{E_g - E_n + \omega_{\text{in}} + i\Gamma}, \quad (6)$$

where $\omega_{\text{in}} \equiv \omega_k - \omega_{\text{res}}$ is the detuning of the incoming photon frequency from resonance and E_n and Γ are the energy and

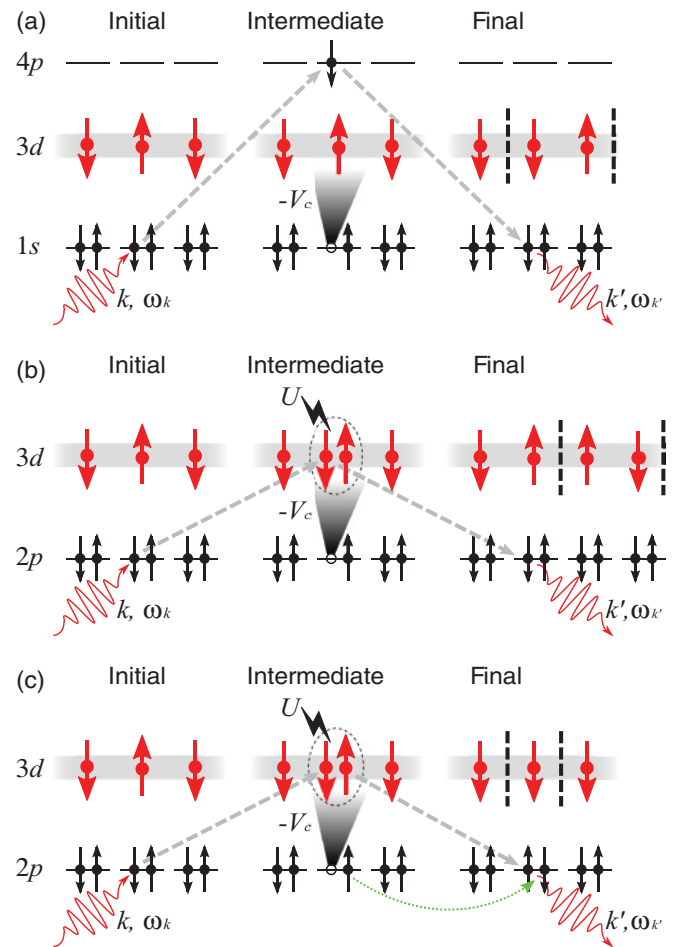


FIG. 1. (Color online) Illustration of RIXS processes in half-filled copper oxides. (a) Indirect RIXS process. (b) Direct RIXS process without spin flip. (c) Direct RIXS process with spin flip. For a spin flip to occur, the core-hole spin must also be flipped (dotted arrow).

lifetime of the intermediate states. The fact that core holes are usually localized allows us to rewrite the above expression as

$$F_{fg}(\omega_{\text{in}}) = \sum_{j\sigma\sigma'} e^{iqR_j} \langle f | d_{j\sigma'} \frac{1}{\hat{H}_j - E_g - \omega_{\text{in}} - i\Gamma} d_{j\sigma}^\dagger | g \rangle, \quad (7)$$

where $q \equiv k - k'$ is the momentum transfer and $\hat{H}_j \equiv \hat{H}_0 - V_c \hat{n}_j$ is a locally perturbed Hamiltonian. For indirect RIXS, one has $d_{j\sigma}^\dagger \equiv 1$, i.e., the only impact of the photon is the creation of the core hole, as illustrated in Fig. 1(a). For direct RIXS, $d_{j\sigma}^\dagger \equiv c_{j\sigma}^\dagger$ photoexcites an electron into the band modeled by the (extended) Hubbard model [see Figs. 1(b) and 1(c)]. In the case of direct RIXS, care must be taken to sum over both the RIXS processes involving a photoexcited up electron and the one involving a down electron because the singlet character of the ground state is otherwise not preserved.

B. Method

We use the Lanczos method^{36,37} to obtain the ground state of finite Hubbard rings and then to evaluate the RIXS

cross section of Eq. (5). Even though the RIXS final state is translationally invariant, the intermediate-state Hamiltonian \hat{H}_j , which is needed to evaluate the Green's functions acting on the initial state, is not. Translational invariance can thus not be used to reduce the Fock space size and all results presented here are for 14-site rings. RIXS spectra of smaller even site, as well as of 16-site rings, have also been selectively calculated and were found to be qualitatively and quantitatively consistent with the 14-site results.

Related numerical calculations of RIXS spectra using a similar method have been carried out³¹ for a few specific cases and the results are in agreement with ours. We use t as unit of energy, the onsite Coulomb repulsion is kept fixed at $U = 10t$, and where the extended Hubbard model is studied, we set $V = 2t$. We have used Lanczos exact diagonalization to explore signature features of the RIXS response and its dependence on the remaining parameters of the Hamiltonian describing the core-hole potential and the energy of the incoming photon.

III. RESULTS

A. Spin excitations in RIXS spectra

The outcome of an indirect RIXS process depends strongly on the resonance condition. Calculation of the x-ray absorption (XAS) spectrum for the Hubbard model shows that there are two main resonances for indirect RIXS (Ref. 38): one corresponds to intermediate states where the valence band at the core-hole site is doubly occupied and the core hole is therefore well-screened, at energies $\sim U - 2V_c$ with respect to the initial state, and the other to states where the core-hole site is singly occupied and the core hole is poorly screened, at energies $\sim -V_c$ with respect to the initial state. In states with double occupancies at the core-hole sites, exchange interactions are not favorable and therefore spin excitations are not pronounced, whereas they are favored when core-hole sites are singly occupied. This is evident in Fig. 2(a), where the low-energy parts of the indirect RIXS spectra taken close to the two resonances are presented.

In direct RIXS, on the other hand, a double occupancy is created at the core-hole site by default at half-filling and therefore there is only one resonance, corresponding to well-screened intermediate states. The form of the RIXS scattering amplitude (7) suggests that in direct RIXS there can be processes where $\sigma = \sigma'$ ($\Delta S = 0$) or $\sigma \neq \sigma'$ ($\Delta S = 1$). In a direct RIXS experiment, both processes take place. For a $\Delta S = 1$ process to occur, however, a spin-orbit interaction between the spin and angular degrees of freedom of the core hole is necessary (see Fig. 1). Hence, the weight ratio of the two direct RIXS processes depends heavily on the strength of the core-hole spin-orbit coupling.

The low-energy parts of the spectra for the two direct RIXS processes are depicted in Figs. 2(b) and 2(c). It is seen that excitations in the low-energy part of the $\Delta S = 0$ process spectrum are almost identical to those occurring in indirect RIXS [Fig. 2(a)], although in this case they are caused by the decoupling of the intermediate-state doublon into an antiholon and a spinon. The $\Delta S = 1$ process spectrum is very similar to the spin dynamical structure factor (DSF) $S(q)$ for the studied system, shown in Figs. 2(d)–2(f), and corresponds mainly to

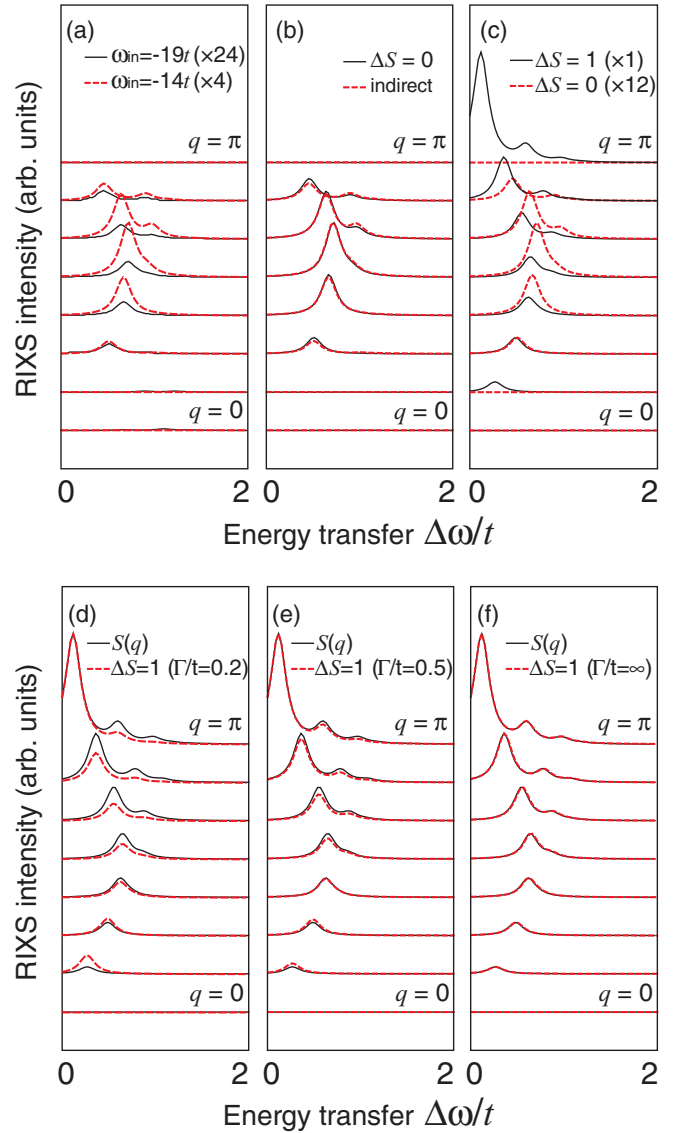


FIG. 2. (Color online) Overview of magnetic excitations in calculated RIXS spectra for the Hubbard model on a half-filled, 14-site ring. The parameters are $U/t = 10$, $V_c/t = 15$, $\omega_{in}/t = -19$, $\Gamma/t = 1$, unless otherwise noted. The peaks are Lorentzians of width $0.1t$. Note that RIXS spectra in (a) and (c) are rescaled by the factors in parentheses. First row: (a) Indirect RIXS spectra for input energies corresponding to well-screened (solid line) and poorly screened (dashed line) intermediate states. (b) $\Delta S = 0$ direct RIXS spectrum (solid line) compared to indirect RIXS (dashed line). (c) $\Delta S = 1$ direct RIXS spectrum (solid line) compared to $\Delta S = 0$ direct RIXS (dashed line). Second row: Spin DSF for the same system (solid line) compared to $\Delta S = 1$ direct RIXS spectrum (dashed line) for (d) $\Gamma/t = 0.2$, (e) $\Gamma/t = 0.5$, and (f) “instant” ($\Gamma/t = \infty$) RIXS process.

single-magnon excitations. Indeed, by setting $\Gamma = 1/\tau \rightarrow \infty$, i.e., by assuming an instantaneous RIXS process with an infinitely fast decay of the core hole, $S(q)$ is obtained exactly [see Fig. 2(f)]. The differences between $S(q)$ and the $\Delta S = 1$ direct RIXS spectrum in Figs. 2(d) and 2(e) are thus a direct consequence of the core hole’s finite lifetime in the intermediate state.

The aforementioned differences between $S(q)$ and the $\Delta S = 1$ direct RIXS spectrum consist of changes in the weight distribution along the Brillouin zone, while the total weight remains constant, as will be shown in the following. Even though the $\Delta S = 1$ direct RIXS spectrum may appear to be almost insensitive to the value of Γ , the effect of a finite core-hole lifetime is actually important for the determination of the line shape, even though the main excitation in a $\Delta S = 1$ direct RIXS process, namely, the single magnon, does not depend on the presence of the core hole. On the contrary, indirect and $\Delta S = 1$ direct RIXS processes depend crucially on core-hole properties (see discussion below).

The generic features of the spectra in Fig. 2 are similar to those found in linear spin-wave theory results,²⁹ but they have more structure. For example, in $\Delta S = 1$ direct RIXS, several peaks arise when moving toward the Brillouin-zone boundary, apart from the single peak of single-magnon excitations. Also, the two-magnon spectral function is found to be finite at the zone boundary using spin-wave theory, but in Figs. 2(b) and 2(c), we see that the $\Delta S = 0$ direct RIXS amplitude vanishes there. This means that two-magnon excitations at $q = \pi$ can arise only in $\Delta S = 1$ direct RIXS. Our results are also consistent with numerical Bethe-ansatz calculations of dynamical spin and spin-exchange structure factors for the Heisenberg model,³² which are the zero-lifetime limits of $\Delta S = 1$ direct and indirect RIXS processes, respectively.

The $\Delta S = 1$ part of the direct RIXS response is one order of magnitude larger than that of the $\Delta S = 0$ process. This is because in the $\Delta S = 1$ case, there will be a magnon excitation in the final state even if no scattering with the core-hole potential occurs in the intermediate state. In the $\Delta S = 0$ case, at least two scatterings of electrons off the core-hole potential are needed for magnetic excitations to arise. In direct RIXS, the incoming photon's angular momentum couples to the core electron's angular momentum, which is in turn coupled to the electron spin via spin-orbit coupling. This implies that it is in principle possible to alter the ratio of the two processes by appropriate choice of the incoming beam polarization and thus observe experimentally the respective change in the character of the spin excitations. An interesting feature seen in Fig. 2(c)

is the difference between the one- and the two-magnon peak locations. This difference decreases with increasing chain length and becomes zero for long chains. The fact that the two RIXS responses scale differently with increasing system size is related to the different size of the excitations present in each case. It is noteworthy that experimental characterization of another quasi-1D cuprate, CaCu_2O_3 , suggests the presence of weakly coupled, finite-size chain segments, 13–14 copper sites in length.³⁹ Such an energy difference might thus reveal signatures of chain breaks, in addition to an analysis of the static magnetic susceptibility.⁴⁰ If this is indeed the case, then our results show that this energy difference can be resolved in direct RIXS experiments and can possibly be used to distinguish the different spin-excitation weights. Before proceeding, we note that all the results presented in Fig. 2 are qualitatively the same and quantitatively very similar for the extended Hubbard model, for values of up to $2t$ for the nearest-neighbor Coulomb repulsion.

B. Resonance condition and detuning

The type of excitations present in the final state of RIXS is defined not only by the type of transition in the absorption step, but also by the position relative to the main resonance peak. By appropriately tuning ω_{in} , specific excitations can thus be favored or hindered. This is evident, for example, in the dependence of the total spin-excitation weight on ω_{in} around the XAS peaks, as presented in Figs. 3(a) and 3(b). The momentum dependence of the charge-sector excitations can be explained within a free particle-hole (doublon-hole) excitation picture and is very similar to that obtained in electron energy-loss spectroscopy (EELS) measurements.⁹ The energy-loss range of charge excitations in RIXS becomes narrower with increasing momentum and the main peak shifts to higher energy loss.³¹ Similar spectral shifts of charge excitation peaks are observed in numerical results for two-dimensional cuprates.^{38,41} A finite nearest-neighbor Coulomb repulsion V is equivalent to an attraction between neighboring doublon-hole pairs and leads to a transfer of charge spectral weight to lower energies for all momenta.³¹ Apart from this shift, the

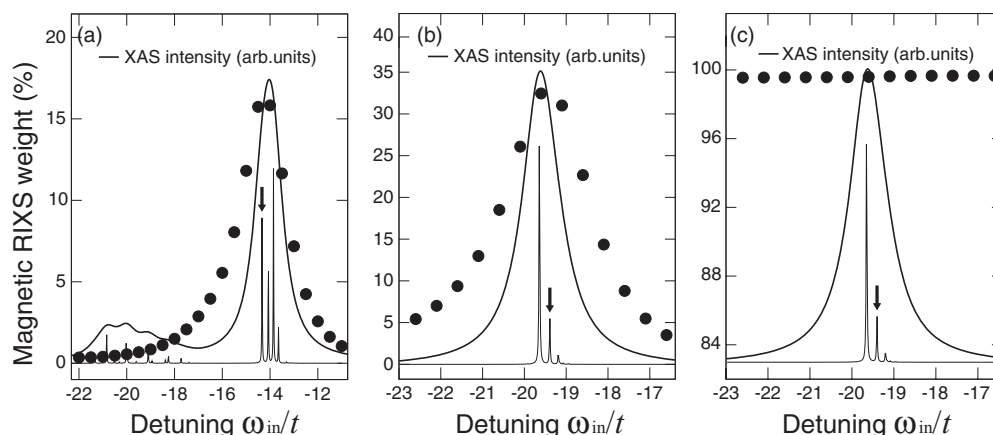


FIG. 3. Total spin-excitation weight, summed over all inequivalent momenta q in the first Brillouin zone, as a function of ω_{in} in (a) indirect, (b) $\Delta S = 0$, and (c) $\Delta S = 1$ direct RIXS, respectively, for the same system as in Fig. 2. The thick (thin) solid lines are the corresponding XAS spectra with Γ_{XAS} set to $0.5t$ ($0.01t$). The arrows indicate the XAS peaks at which the magnetic RIXS signal is maximal.

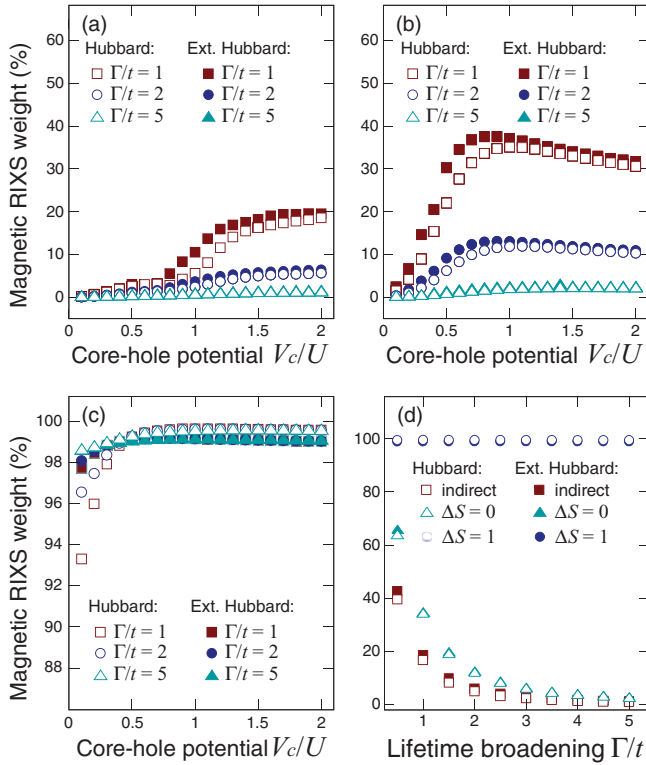


FIG. 4. (Color online) Total spin-excitation weight percentage as a function of the core-hole potential in (a) indirect RIXS, (b) $\Delta S = 0$ direct RIXS, and (c) $\Delta S = 1$ direct RIXS for Hubbard (empty symbols) and extended Hubbard (full symbols) models, for three values of the inverse lifetime Γ . The value for the detuning ω_{in} of the incoming photon energy from resonance at each point is defined by the procedure outlined in the text. All other relevant parameters are as in Fig. 2. (d) Core-hole lifetime dependence of magnetic excitations in all RIXS processes for $V_c = 15t$.

results presented in Fig. 3 remain qualitatively unchanged for values of up to $V = 2t$.

It is noted that the maxima of absorption in Figs. 3(a) and 3(b) do not coincide exactly with the maxima of spin excitations. Upon increasing the XAS spectrum resolution, it is seen that the maximal RIXS spin excitation response lies close to specific states within the broad peaks. Therefore, in order to study the dependence of excitations on the core-hole potential strength, ω_{in} must be carefully selected in each case. For this purpose, the ω_{in} dependence of the spectrum is investigated first for each value of V_c , and the value that yields the largest spin-excitation weight is chosen as a reference. For example, the arrows in Fig. 3 point to the appropriate ω_{in} values for the case of $V_c = 15t$. After determining the reference states, the V_c dependence of the total weights can be studied. The scaling of the total magnetic excitation weight, summed over all inequivalent momenta in the first Brillouin zone, is shown in Fig. 4 for indirect and direct RIXS processes.

C. Role of the core-hole potential magnitude

Figure 4 shows the relative spin-excitation spectral weight as a function of the core-hole potential for three different core-hole lifetime values. As was mentioned above, the

experimental direct RIXS spectra contain both the $\Delta S = 0$ and 1 contributions. It is in principle possible to deduce the contribution of each of the two processes by comparing the momentum dependence of the experimental spectrum line shape (with all geometrical factors stripped off) to the line shapes of Figs. 2(b) and 2(c). One can then compare with the results presented in Fig. 4 and determine possible values for the core-hole potential and lifetime, which are typically considered as fit parameters. We note that this estimation scheme is general and therefore applicable to more complicated models, provided that the spin excitations can be clearly distinguished from other excitations, such as, e.g., $d-d$ excitations in multiple-orbital models.

The spin-excitation weight for indirect RIXS in Fig. 4(a) shows a dip around $V_c = U$ for both Hubbard and extended Hubbard models. This can be intuitively understood as follows: for these values of the core-hole potential, the attraction exerted by the core hole to an electron on a different site is approximately canceled by the effect of the onsite Coulomb repulsion due to the electron already occupying the site with the core hole. There is therefore no cause for scattering, and spin-exchange processes are consequently suppressed. We find no such dip in $\Delta S = 0$ direct RIXS, a fact which demonstrates the different origin of the same excitations in the two RIXS processes. As can be seen in Fig. 4, the inclusion of a nearest-neighbor Coulomb repulsion with $V/t = 2$ does not substantially alter spin-excitation weights.

D. RIXS core-hole lifetime

It has been noticed in previous studies that the value of the intermediate-state lifetime $1/\Gamma$ affects the weight of spin excitations in model calculations.³⁴ The reason is that spin-exchange processes are slow compared to charge excitations. This is indeed the case for indirect RIXS. In direct RIXS, however, the single-spin flip is, as discussed above, a zero-order process in terms of electron–core-hole scattering, and the total excitation weight does therefore not depend on ω_{in} , Γ , or V_c , even though the line shape depends on these parameters, as is shown in Figs 2(d)–2(f) for the case of Γ . This implies that in direct RIXS, evidence of single-spin excitations should be experimentally observable in 1D chain materials, as is the case at the Cu L edge in 2D cuprates^{20,21} and in $\text{Sr}_{14}\text{Cu}_{24}\text{O}_{41}$.¹⁹ Regarding the double spin-flip processes in RIXS, the core-hole lifetime has been shown to be sufficient to detect such spin excitations in the case of the the Cu K edge in 2D cuprates.^{20,42} It is thus justified to assume that the intermediate-state lifetime is similarly long enough in chain systems, suggesting that spin excitations due to exchange interactions should be present in experimental RIXS spectra.

As can be seen in Figs. 4(a)–4(c), magnetic excitation weights remain unchanged for large ranges of V_c , in both direct and indirect RIXS. Since it is very likely that the physical value of the core-hole attraction is within these ranges, the core-hole lifetime dependence of magnetic excitations shown in Fig. 4(d) can be used to identify the lifetime range corresponding to experimental observations. The currently used estimates based on the XAS core-hole lifetime, as well as experimental RIXS evidence,⁴³ suggest that $\Gamma/t < 1$, a fact that underlines the significance of the effects of the finite core-hole lifetime

presented above. This approach to obtain core-hole lifetimes is usable even in cases where the lifetime does not correspond to the natural linewidth. In the future, it may thus become particularly useful for the interpretation of time-resolved RIXS measurements, in which the intermediate-state lifetime will be controlled via stimulated emission.

IV. CONCLUSIONS

We have determined the direct and indirect RIXS responses of the half-filled, single-band Hubbard model in one dimension by using exact diagonalization, systematically varying relevant parameters. In the low-energy sector, our results exhibit the main magnetic excitations allowed theoretically, namely, two-magnon excitations in the indirect and $\Delta S = 0$ direct RIXS processes and single-magnon excitations in $\Delta S = 1$ processes. The strong dependence of the total spin-excitation weight on the resonance condition, as well as on the detuning from resonance, is apparent in the RIXS spectra. The characteristics of spin excitations in all RIXS processes remain qualitatively unchanged by the introduction of a nearest-neighbor Coulomb repulsion with magnitude of up to $2t$. The general features of the calculated spectra are accessible to experiment, and it is of interest to see to what extent the obtained generic results can describe measured magnetic features of 1D single-chain cuprates, which have yet to appear.

Furthermore, we have studied the dependence of spin excitations created by RIXS on the strength of the core-hole potential, and we have presented a method for estimating the core-hole properties of interest using our or equivalent results, in conjunction with the respective geometrical factors. It is also seen that spin excitations in indirect RIXS are suppressed for values of V_c close to the onsite Coulomb repulsion strength U due to suppression of electron scattering off the core hole. The total weight of magnetic excitations in $\Delta S = 1$ direct RIXS does not depend on incoming photon energy, core-hole potential magnitude, or core-hole lifetime, and can be used as a reference by which the total $\Delta S = 0$ contribution can be distinguished in experimental data. Using the ratio of the magnetic weights, the core-hole properties can be estimated.

During the writing of this paper, a preprint by Igarashi and Nagao appeared⁴⁴ in which they apply their previously developed formalism⁴⁵ to 1D systems and obtain similar results to those in Fig. 2.

ACKNOWLEDGMENTS

The authors are grateful to L. Ament, V. Bisogni, and K. Wohlfeld for invaluable discussions. This work was supported by the Deutsche Forschungsgemeinschaft under the Emmy-Noether program (S.K. and M.D.).

¹E. Lieb and F. Wu, *Phys. Rev. Lett.* **20**, 1445 (1968).

²N. Motoyama, H. Eisaki, and S. Uchida, *Phys. Rev. Lett.* **76**, 3212 (1996).

³M. Matsuda, K. Katsumata, K. M. Kojima, M. Larkin, G. M. Luke, J. Merrin, B. Nachumi, Y. J. Uemura, H. Eisaki, N. Motoyama, S. Uchida, and G. Shirane, *Phys. Rev. B* **55**, R11953 (1997).

⁴A. Keren, L. P. Le, G. M. Luke, B. J. Sternlieb, W. D. Wu, Y. J. Uemura, S. Tajima, and S. Uchida, *Phys. Rev. B* **48**, 12926 (1993).

⁵K. Kojima, M. Larkin, G. M. Luke, B. Nachumi, Y. J. Uemura, H. Eisaki, M. Motoyama, S. Uchida, B. J. Sternlieb, and G. Shirane, *Czech. J. Phys.* **46**, 1945 (1996).

⁶K. M. Kojima, Y. Fudamoto, M. Larkin, G. M. Luke, J. Merrin, B. Nachumi, Y. J. Uemura, N. Motoyama, H. Eisaki, S. Uchida, K. Yamada, Y. Endoh, S. Hosoya, B. J. Sternlieb, and G. Shirane, *Phys. Rev. Lett.* **78**, 1787 (1997).

⁷C. Kim, A. Y. Matsuura, Z.-X. Shen, N. Motoyama, H. Eisaki, S. Uchida, T. Tohyama, and S. Maekawa, *Phys. Rev. Lett.* **77**, 4054 (1996).

⁸C. Kim, Z.-X. Shen, N. Motoyama, H. Eisaki, S. Uchida, T. Tohyama, and S. Maekawa, *Phys. Rev. B* **56**, 15589 (1997).

⁹R. Neudert, M. Knupfer, M. S. Golden, J. Fink, W. Stephan, K. Penc, N. Motoyama, H. Eisaki, and S. Uchida, *Phys. Rev. Lett.* **81**, 657 (1998).

¹⁰B. J. Kim, H. Koh, E. Rotenberg, S.-J. Oh, H. Eisaki, N. Motoyama, S. Uchida, T. Tohyama, S. Maekawa, Z.-X. Shen, and C. Kim, *Nat. Phys.* **2**, 397 (2006).

¹¹L. Ament, M. van Veenendaal, T. Devereaux, J. Hill, and J. van den Brink, *Rev. Mod. Phys.* **83**, 705 (2011).

¹²J. van den Brink and M. van Veenendaal, *J. Phys. Chem. Solids* **66**, 2145 (2005).

¹³J. van den Brink and M. van Veenendaal, *Europhys. Lett.* **73**, 121 (2006).

¹⁴M. Z. Hasan, P. A. Montano, E. D. Isaacs, Z.-X. Shen, H. Eisaki, S. K. Sinha, Z. Islam, N. Motoyama, and S. Uchida, *Phys. Rev. Lett.* **88**, 177403 (2002).

¹⁵Y.-J. Kim, J. P. Hill, H. Benthien, F. H. L. Essler, E. Jeckelmann, H. S. Choi, T. W. Noh, N. Motoyama, K. M. Kojima, S. Uchida, D. Casa, and T. Gog, *Phys. Rev. Lett.* **92**, 137402 (2004).

¹⁶D. Qian, Y. Li, M. Hasan, D. Casa, T. Gog, Y. Chuang, K. Tsutsui, T. Tohyama, S. Maekawa, and H. Eisaki, *J. Phys. Chem. Solids* **66**, 2212 (2005).

¹⁷S. Suga, S. Imada, A. Higashiya, A. Shigemoto, S. Kasai, M. Sing, H. Fujiwara, A. Sekiyama, A. Yamasaki, C. Kim, T. Nomura, J. Igarashi, M. Yabashi, and T. Ishikawa, *Phys. Rev. B* **72**, 081101 (2005).

¹⁸J. W. Seo, K. Yang, D. W. Lee, Y. S. Roh, J. H. Kim, H. Eisaki, H. Ishii, I. Jarrige, Y. Q. Cai, D. L. Feng, and C. Kim, *Phys. Rev. B* **73**, 161104 (2006).

¹⁹J. Schlappa, T. Schmitt, F. Vernay, V. N. Strocov, V. Ilakovac, B. Thielemann, H. M. Rønnow, S. Vanishri, A. Piazzalunga, X. Wang, L. Braicovich, G. Ghiringhelli, C. Marin, J. Mesot, B. Delley, and L. Patthey, *Phys. Rev. Lett.* **103**, 047401 (2009).

²⁰J. P. Hill, G. Blumberg, Y.-J. Kim, D. S. Ellis, S. Wakimoto, R. J. Birgeneau, S. Komiya, Y. Ando, B. Liang, R. L. Greene, D. Casa, and T. Gog, *Phys. Rev. Lett.* **100**, 097001 (2008).

²¹L. Braicovich, J. van den Brink, V. Bisogni, M. M. Sala, L. J. P. Ament, N. B. Brookes, G. M. De Luca, M. Salluzzo, T. Schmitt, V. N. Strocov, and G. Ghiringhelli, *Phys. Rev. Lett.* **104**, 077002 (2010).

- ²²J. Kim, D. Casa, M. H. Upton, T. Gog, Y.-J. Kim, J. F. Mitchell, M. V. Veenendaal, M. Daghofer, J. van den Brink, G. Khaliullin, and B. J. Kim, e-print [arXiv:1110.0759](https://arxiv.org/abs/1110.0759).
- ²³M. van Veenendaal, e-print [arXiv:1106.0640](https://arxiv.org/abs/1106.0640).
- ²⁴J. Schlappa, K. Wohlfeld, K. J. Zhou, M. Mourigal, M. W. Haverkort, V. N. Strocov, L. Hozoi, C. Monney, S. Nishimoto, S. Singh, A. Revcolevschi, J. S. Caux, L. Patthey, H. M. Rønnow, J. van den Brink, and T. Schmitt (unpublished).
- ²⁵J. van den Brink, *Europhys. Lett.* **80**, 47003 (2007).
- ²⁶L. J. P. Ament, F. Forte, and J. van den Brink, *Phys. Rev. B* **75**, 115118 (2007).
- ²⁷T. Nagao and J. I. Igarashi, *Phys. Rev. B* **75**, 214414 (2007).
- ²⁸L. J. P. Ament, G. Ghiringhelli, M. M. Sala, L. Braicovich, and J. van den Brink, *Phys. Rev. Lett.* **103**, 117003 (2009).
- ²⁹M. W. Haverkort, *Phys. Rev. Lett.* **105**, 167404 (2010).
- ³⁰S. Glawion, J. Heidler, M. W. Haverkort, L. C. Duda, T. Schmitt, V. N. Strocov, C. Monney, K. J. Zhou, A. Ruff, M. Sing, and R. Claessen, *Phys. Rev. Lett.* **107**, 107402 (2011).
- ³¹K. Tsutsui, T. Tohyama, and S. Maekawa, *Phys. Rev. B* **61**, 7180 (2000).
- ³²A. Klauser, J. Mossel, J.-S. Caux, and J. van den Brink, *Phys. Rev. Lett.* **106**, 157205 (2011).
- ³³F. Forte, M. Cuoco, C. Noce, and J. van den Brink, *Phys. Rev. B* **83**, 245133 (2011).
- ³⁴K. Okada and A. Kotani, *J. Phys. Soc. Jpn.* **75**, 044702 (2006).
- ³⁵H. A. Kramers and W. Heisenberg, *Z. Phys.* **31**, 681 (1925).
- ³⁶C. Lanczos, *J. Res. Natl. Bur. Stand. (US)* **45**, 255 (1950).
- ³⁷C. Lanczos, *J. Res. Natl. Bur. Stand. (US)* **49**, 33 (1952).
- ³⁸K. Tsutsui, T. Tohyama, and S. Maekawa, *Phys. Rev. Lett.* **83**, 3705 (1999).
- ³⁹V. Kiryukhin, Y. J. Kim, K. J. Thomas, F. C. Chou, R. W. Erwin, Q. Huang, M. A. Kastner, and R. J. Birgeneau, *Phys. Rev. B* **63**, 144418 (2001).
- ⁴⁰J. Sirker, N. Laflorencie, S. Fujimoto, S. Eggert, and I. Affleck, *Phys. Rev. Lett.* **98**, 137205 (2007).
- ⁴¹C. J. Jia, C.-C. Chen, A. P. Sorini, B. Moritz, and T. P. Devereaux, e-print [arXiv:1109.3446](https://arxiv.org/abs/1109.3446).
- ⁴²V. Bisogni, L. Simonelli, L. J. P. Ament, F. Forte, M. M. Sala, M. Minola, S. Huotari, J. van den Brink, G. Ghiringhelli, N. B. Brookes, and L. Braicovich, e-print [arXiv:1010.4725](https://arxiv.org/abs/1010.4725).
- ⁴³V. Bisogni (private communication).
- ⁴⁴J. Igarashi and T. Nagao, *Phys. Rev. B* **85**, 064422 (2012).
- ⁴⁵J. Igarashi and T. Nagao, *Phys. Rev. B* **85**, 064421 (2012).